

Analyticity constraints bound the decay of the spectral form factor

Pablo Martinez-Azcona  and Aurélia Chenu 

Department of Physics and Materials Science, University of Luxembourg, L-1511 Luxembourg

Quantum chaos cannot develop faster than $\lambda \leq 2\pi/(\hbar\beta)$ for systems in thermal equilibrium [Maldacena, Shenker & Stanford, JHEP (2016)]. This ‘MSS bound’ on the Lyapunov exponent λ is set by the width of the strip on which the regularized out-of-time-order correlator is analytic. We show that similar constraints also bound the decay of the spectral form factor (SFF), that measures spectral correlation and is defined from the Fourier transform of the two-level correlation function. Specifically, the *inflection exponent* η , that we introduce to characterize the early-time decay of the SFF, is bounded as $\eta \leq \pi/(2\hbar\beta)$. This bound is universal and exists outside of the chaotic regime. The results are illustrated in systems with regular, chaotic, and tunable dynamics, namely the single-particle harmonic oscillator, the many-particle Calogero-Sutherland model, an ensemble from random matrix theory, and the quantum kicked top. The relation of the derived bound with other known bounds, including quantum speed limits, is discussed.

1 Introduction

How fast can a given quantum system evolve? Bounds setting limits on the evolution of dynamical quantities have proven to be useful tools and brought a great deal of insight. On the one hand, quantum speed limits, that determine the minimum time for evolution under quantum dynamics [1–5], have been the focus of intense studies in both the quantum [6–10] and classical [11–13] realms, with a recent unification of the two realms for speed limits on observables [14]. Beyond their fundamental relevance, these bounds have become useful tools in the study of quantum

information and technologies [15–17], many-body physics [18–20], and find applications in quantum control [10, 21, 22] and quantum metrology [23, 24].

On another hand, a universal bound on quantum chaotic dynamics has been recently proposed [25]. It sets a limit on the quantum Lyapunov exponent λ , defined from the ‘Out-of-Time-Order Correlator’ (OTOC). This correlator was originally proposed in the context of superconductivity [26] and has been extended to the high energy [27–31] and quantum information [32–43] communities. In the semiclassical limit and for a certain time range, the OTOC behaves exponentially and defines a proper analog of the Lyapunov exponent [44]. Maldacena, Shenker and Stanford [25] conjectured that, for any thermal state, this exponent is bounded as $\lambda \leq 2\pi/(\hbar\beta)$. This finding motivated considerable attention within the community [31, 45–50]. The original derivation relied on the analytic continuation of the regularized OTOC to complex times $t + i\tau$ and the region in which it is analytic, and has been proven alternatively since then [46]. The bound itself has been extended beyond quantum chaos and linked to the fluctuation-dissipation theorem [34, 51]. Similar arguments based on analyticity have yielded bounds on other dynamical quantities [52] or been used to characterize dynamical phase transitions [53].

Here, we show that the mathematical property used to derive the MSS bound applies to quantities other than the OTOC, and sets bounds that are not restricted to chaotic behavior. Particularly, we find these bounds on a dynamical quantity that measures spectral correlation and is very widespread in the quantum chaos community, the spectral form factor [17, 54–58].

In Section 2, we show that the region of analyticity also imposes a universal bound on its early-time evolution, that holds for any system

ranging from regular to chaotic behavior, and can be very tight. We thus also extend such universal bounds beyond the context of quantum chaos, and propose an interpretation of the quantity we bound in terms of the average energy at complex temperature. Section 3 illustrates our findings in systems that are conceptually very different and representatives of regular and chaotic dynamics: the harmonic oscillator, the Calogero-Sutherland model, the Gaussian Unitary Ensemble from random matrix theory [59] and the quantum kicked top [60], which is one of the earliest model introduced to study chaos and can mimic the behavior of any members of a universality class displayed by random matrix theory. In Section 4, we show how the derived bound compares to known bounds, starting with quantum speed limits.

2 A bound on the decay of the spectral form factor

In this Section, we find that the spectral form factor, after the short-time Gaussian decay, decays exponentially with an exponent bounded by the temperature and Planck constant only. The mathematical proof follows that used by MSS [25] and extends its range of applicability to short times, with no neglected terms.

2.1 Early-time decay of the SFF

The spectral form factor (SFF) is an efficient tool for determining the spectral properties of a system, and it is the simplest nontrivial measure of spectral correlations [61]. This dynamical quantity is the Fourier transform of the two-level correlation function and can be interpreted as the fidelity between a coherent Gibbs state [17, 62–65], $|\psi_\beta\rangle = Z_\beta^{-1/2} \sum_n e^{-\beta E_n/2} |n\rangle$, and its time evolution, namely

$$S_{\beta,t} = |\langle \psi_\beta | e^{-\frac{i}{\hbar} \hat{H} t} | \psi_\beta \rangle|^2 = \left| \frac{Z_{\beta+it/\hbar}}{Z_\beta} \right|^2, \quad (1)$$

$$= \frac{1}{Z_\beta^2} \sum_{m,n} e^{-(\beta+\frac{i}{\hbar}t)E_n} e^{-(\beta-\frac{i}{\hbar}t)E_m}.$$

It reads as the normalized analytical continuation of the partition function with $Z_\beta = \text{Tr}(e^{-\beta \hat{H}}) = \sum_n e^{-\beta E_n}$, E_n being the system eigenenergies and β the inverse temperature. The SFF decays from its initial unity value with a Gaussian

shape at short times [17]. For systems with correlated eigenenergies such as chaotic ones, the SFF reaches a dip and then goes up with a ramp, interpreted as a signature of chaos [17, 57, 58], and plateaus at a constant value, fixed by the dimension of the Hilbert space N and the temperature.

While the SFF is widely used in chaos because of this characteristic shape, we are here interested in its early-time decay, that is, after the initial Gaussian decay and before the onset of chaotic features. We are thus not restricting ourselves to any dynamical regime. Specifically, we consider the time t_0 at which $\ln(S_{\beta,t})$ has a first inflection point—its second derivative vanishes. To characterize the decay around this time, we introduce the *inflection exponent*

$$\eta = \left| \frac{\dot{S}_{\beta,t_0}}{S_{\beta,t_0}} \right|, \quad (2)$$

that corresponds to $\max_t |\dot{S}_{\beta,t}/S_{\beta,t}|$. Around this time maximum, the function can be approximated by a constant up to first order in time, *i.e.* $|\dot{S}_{\beta,t}/S_{\beta,t}| = \eta + \mathcal{O}((t-t_0)^2)$. So for t close to t_0 , the SFF decays exponentially $S_{\beta,t} \sim S_{\beta,0}^0 e^{-\eta t}$, with $S_{\beta,0}$ a constant. We find that this early-time decay of the SFF is actually bounded.

2.2 Bound on the SFF exponential decay

The proof that η is bounded is sketched in Fig. 1. We rely on the analytical continuation of the SFF to complex times, that we define as

$$S_{\beta,t+i\tau} = \frac{Z_{\beta-\tau/\hbar+it/\hbar} Z_{\beta+\tau/\hbar-it/\hbar}}{Z_\beta^2}, \quad (3)$$

and tools from complex analysis. Specifically, we use the *Schwarz-Pick theorem*: For an analytic¹ function f_z of a complex variable $z = x + iy$ that maps the unit disk \mathcal{D} into itself $f_z : z \in \mathcal{D} \rightarrow \mathcal{D}$, the following inequality holds

$$\frac{|df_z|}{1-|f_z|^2} \leq \frac{|dz|}{1-|z|^2}, \quad (4)$$

with the differentials $df_z = \frac{\partial f_z}{\partial x} dx + \frac{\partial f_z}{\partial y} dy$ and $dz = dx + idy$. Note that the condition of mapping the unit disk into itself is equivalent to satisfying $|f_z| \leq 1 \forall z \in \mathcal{D}$.

¹A function of a complex variable f_z is analytic in a region \mathcal{R} if it can be written as a power series convergent at every point of \mathcal{R} .

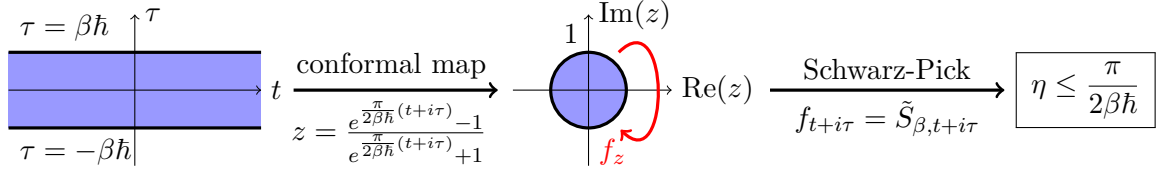


Figure 1: **Illustration of the proof that bounds the inflection exponent η .** From left to right: The strip (t, τ) of the complex plane in which $f_{t+i\tau}$ is analytic is mapped to the unit disk using the conformal map (5). For an analytic function f_z that maps z from the unit disk to f_z onto the same unit disk and fulfills $|f_z| \leq 1$, the Schwarz-Pick theorem yields a bound on f_z (4). For the spectral form factor, this results in a bound on the inflection exponent that is fixed by the system temperature and the Planck constant, see Eq. (9).

The spectral form factor at complex time, $t \rightarrow t + i\tau$ see Eq. (3), is analytic on the strip of the complex plane $-\beta\hbar \leq \tau \leq +\beta\hbar$ and $t \in \mathbb{R}$, as shown in App. A. This strip holds for systems with a Hilbert space of infinite dimension with unbounded energies, as well as for systems with a finite-dimensional Hilbert space—in this latter case, the SFF is analytic on the whole complex plane² because it is given by a finite linear combination of complex exponentials, analytic on the whole complex plane. In contrast to quantities like the OTOC or two-point correlation functions, this quantity is also analytic at $t = 0$, as we verify in App. A.

The region in which the SFF is analytic can be mapped to the unit disk using

$$z = \frac{e^{\frac{\pi}{2\beta\hbar}(t+i\tau)} - 1}{e^{\frac{\pi}{2\beta\hbar}(t+i\tau)} + 1}. \quad (5)$$

Using inequality (4) along the real line $\tau = 0$ yields

$$\frac{1}{1 - |f_t|^2} \left| \frac{df_t}{dt} \right| \leq \frac{1}{2} \frac{\pi}{2\beta\hbar}, \quad (6)$$

which, assuming $f_t \in \mathbb{R}$ in the real line t , can be recasted as

$$\frac{1}{1 - f_t} \left| \frac{df_t}{dt} \right| \leq \frac{1 + f_t}{2} \frac{\pi}{2\beta\hbar} \leq \frac{\pi}{2\beta\hbar}. \quad (7)$$

This inequality is very similar to the one used by MSS [25] but with one difference, which is key to derive bounds at short times: the terms $\mathcal{O}(e^{-4\pi t/(\beta\hbar)})$ are not neglected. These terms could be important at early times and therefore analyticity at $t = 0$ plays an important role.

²As is also stated in [53] for the analytical continuation of the partition function, we find that the SFF is an entire function (analytic in the whole complex plane) of z for a finite dimensional Hilbert space.

Importantly, we need $|f_z| \leq 1$ in all points of the domain to obtain the inequality (4) from the Schwarz-Pick theorem. To do so, we define the *modified spectral form factor*,

$$\tilde{S}_{\beta,t+i\tau} = 1 - \frac{Z_{\beta-\frac{\tau}{\hbar}+\frac{i}{\hbar}t} Z_{\beta+\frac{\tau}{\hbar}-\frac{i}{\hbar}t}}{Z_{\beta-\frac{\tau}{\hbar}} Z_{\beta+\frac{\tau}{\hbar}}} \quad (8)$$

that we introduce such that $\tilde{S}_{\beta,t} = 1 - S_{\beta,t}$ on the real line and, since $|Z_{\beta-\frac{\tau}{\hbar}+\frac{i}{\hbar}t} Z_{\beta+\frac{\tau}{\hbar}-\frac{i}{\hbar}t}| \leq Z_{\beta-\frac{\tau}{\hbar}} Z_{\beta+\frac{\tau}{\hbar}}$, one expects $|\tilde{S}_{\beta,t+i\tau}| \leq 1$ —there is however a subtlety that we discuss in the next subsection. Note that this function still preserves analyticity in the same domain, since the denominator is an analytic function that is never zero and the numerator is analytic on the strip (as shown in App. A). This function has the same inflection exponent that the SFF and fulfills the conditions to apply the Schwarz-Pick theorem. Choosing f_z to be the modified SFF, $f_{t+i\tau} = \tilde{S}_{\beta,t+i\tau}$, the l.h.s. of inequality (7) simplifies and we obtain a bound on the inflection exponent:

$$\eta \leq \frac{\pi}{2\beta\hbar}. \quad (9)$$

This is our main result. It means that around the inflection time t_0 , the fastest possible decay of the SFF is proportional to the temperature of the system.

2.3 Bound for an extensive inflection exponent

Note that Eq. (9) holds provided that η is intensive. However, this need not always be the case since, in the most general case, the partition function $Z_\beta = e^{-\beta F}$ is defined from the Helmholtz free energy F , which can be extensive. Since η represents the exponential decay of the SFF that is defined from the partition function, it is expected to be extensive whenever F is extensive. Whenever η is extensive is some quantity d (e.g. the

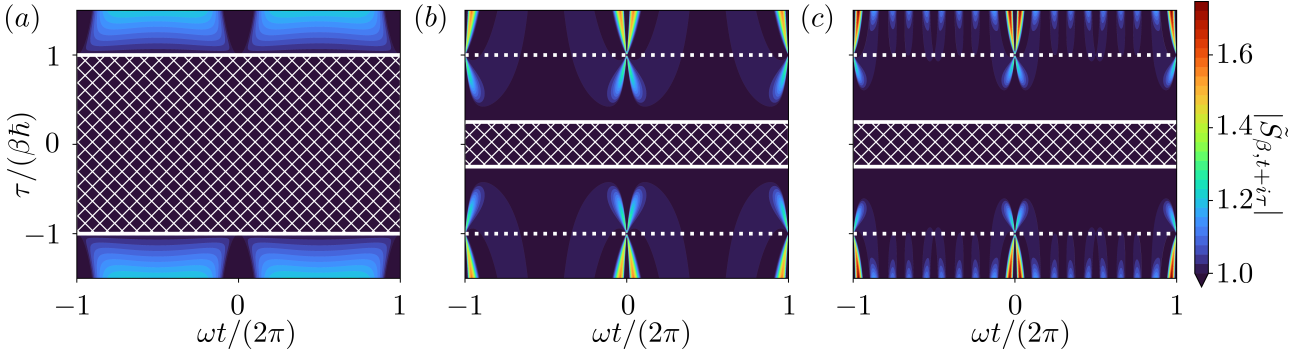


Figure 2: **Modulus of the modified Spectral Form Factor for complex time** $|\tilde{S}_{\beta,t+i\tau}|$ for (a) a single harmonic oscillator, (b) a set of independent harmonic oscillators with partition function $Z_\beta = (Z_\beta^{\text{HO}})^N$ and (c) the Calogero-Sutherland model. The scale has been chosen to highlight the regions in which $|\tilde{S}_{\beta,t+i\tau}| > 1$. For both (b) and (c) $N = 4$ particles were considered. The dotted white lines represent the standard strip $-\beta\hbar \leq \tau \leq \beta\hbar$ and the solid lines with the hatch represent the renormalized strip $-\beta\hbar/N \leq \tau \leq \beta\hbar/N$. The function is bounded in this renormalized strip, $|\tilde{S}_{\beta,t+i\tau}| \leq 1$, where the Schwarz-Pick theorem holds.

dimension of the system, the number of particles, or the central charge in conformal field theory), we conjecture a correction of the bound as

$$\frac{\eta}{d} \leq \frac{\pi}{2\beta\hbar}. \quad (10)$$

The idea behind this correction is that the modulus of the modified SFF $|\tilde{S}_{\beta,t+i\tau}|$ can be bigger than unity in the strip $-\beta\hbar \leq \tau \leq \beta\hbar$ for the models in which η is extensive. A way to recover the condition that f_z maps the unit disk into itself is to shrink the strip to $-\beta\hbar/d \leq \tau \leq \beta\hbar/d$. Substituting $\beta \rightarrow \beta/d$ in (9) yields the bound for an extensive inflection exponent given in Eq. (10).

Figure 2 illustrates the correction of the strip for N independent harmonic oscillators and for the Calogero Sutherland model. In both cases, $|\tilde{S}_{\beta,t+i\tau}|$ is bigger than one for some regions of the original strip but not within the shrunk strip, so the Schwarz-Pick theorem applies. This conjecture is further detailed in Sec. 3.2 for the Calogero-Sutherland model, that is extensive in the number of particles.

2.4 An interpretation of the inflection exponent

The spectral form factor (1) can be written as the expectation value of the evolution operator $\hat{U}_t = e^{-i\hat{H}t/\hbar}$ for the thermal state $\hat{\rho}_\beta = e^{-\beta\hat{H}}/Z_\beta$, that is, $S_{\beta,t} = \langle \hat{U}_t \rangle_\beta \langle \hat{U}_t^\dagger \rangle_\beta$ where $\langle \bullet \rangle_\beta = \text{Tr}(\bullet \hat{\rho}_\beta)$.

Thus,

$$\frac{\dot{S}_{\beta,t}}{S_{\beta,t}} = -\frac{i}{\hbar} \frac{\langle \hat{H} \hat{U}_t \rangle_\beta}{\langle \hat{U}_t \rangle_\beta} + \frac{i}{\hbar} \frac{\langle \hat{H} \hat{U}_t^\dagger \rangle_\beta}{\langle \hat{U}_t^\dagger \rangle_\beta}. \quad (11)$$

The inflection exponent, as defined in (2), corresponds to this expression evaluated at the inflection time t_0 , *i.e.* when the function has its first minimum. Since the two terms in (11) are complex conjugates of each other, the inflection exponent η can be recast as

$$\eta = \frac{2}{\hbar} \text{Im} \left(\frac{\langle \hat{H} \hat{U}_{t_0}^\dagger \rangle_\beta}{\langle \hat{U}_{t_0}^\dagger \rangle_\beta} \right) = \frac{2}{\hbar} \text{Im} \langle \hat{H} \rangle_{\beta - \frac{i}{\hbar} t_0}, \quad (12)$$

which corresponds to the imaginary part of the average energy at complex β , where the complex part of the inverse temperature is fixed by the inflection time t_0 . Note that, when dealing with chaotic systems defined over an ensemble, the value of the inflection time t_0 cannot be determined from a single realization but rather from the averaged SFF. This is because the SFF is not self-averaging [66], as we detail in the examples below. In this case, the above definition (12) is not computationally efficient unless exact analytic forms of $\langle \hat{H} \rangle_\beta$ are known.

Finally, the derived bound poses the maximum value

$$\text{Im} \left(\frac{\langle \hat{H} \hat{U}_{t_0}^\dagger \rangle_\beta}{\langle \hat{U}_{t_0}^\dagger \rangle_\beta} \right) = \text{Im} \langle \hat{H} \rangle_{\beta - \frac{i}{\hbar} t_0} \leq \frac{\pi}{4\beta}. \quad (13)$$

This interpretation of the inflection exponent highlights that the initial Gaussian decay, determined by $\Delta \hat{H}^2$ [17], is followed by the early-time exponential decay with a different exponent,

which is determined by the imaginary part of the expectation value of \hat{H} at complex β .

3 Examples

In order to illustrate the derived bound in some specific setups, we choose four conceptually very different systems, that respectively exhibit regular (both single- and many-particle), chaotic, and tunable (between regular and chaotic) dynamics. Namely, we compute the SFF and look at the inflection exponent in the harmonic oscillator, the Calogero-Sutherland model, an ensemble from random matrix theory, and the quantum kicked top.

3.1 Integrable system: the harmonic oscillator

We start with a single particle in an harmonic trap, which Hamiltonian

$$\hat{H} = \hbar\omega \left(\hat{a}^\dagger \hat{a} + \frac{1}{2} \right) \quad (14)$$

is expressed in terms of annihilation and creation operators, \hat{a} and \hat{a}^\dagger , and has eigenenergies $E_n = \hbar\omega(n + 1/2)$. This system represents one of the simplest integrable models. The analytically continued partition function, $Z_{\beta+it} = \left(2 \sinh[(\beta\hbar + it)\omega/2] \right)^{-1}$, gives the SFF as

$$S_{\beta,t}^{\text{HO}}(\omega) = \frac{\cosh(\beta\hbar\omega) - 1}{\cosh(\beta\hbar\omega) - \cos(\omega t)}. \quad (15)$$

The system energies have a constant spacing, so the SFF, shown in Fig. 3(a), is a periodic function—of period $2\pi/\omega$. As the system temperature is increased, the SFF minimum, equal to $\tanh^2(\beta\hbar\omega/2)$, decreases. We verify that $e^{-\eta t}$ constitutes a good approximation around t_0 to characterize the decay of the SFF after the initial Gaussian decay.

In order to obtain the inflection exponent η , defined in Eq. (2), we look for the time t_0 at which $\frac{\dot{S}}{S} = -\frac{\omega \sin(\omega t)}{\cosh(\beta\hbar\omega) - \cos(\omega t)}$ has an extremum. This gives the exponent as

$$\eta_\beta^{\text{HO}}(\omega) = \frac{\omega}{\sinh(\beta\hbar\omega)} = 2\omega Z_{2\beta}. \quad (16)$$

This inflection exponent gets closer to the $\pi/(2\hbar\beta)$ bound (9) at high temperature, with an asymptote at $1/\hbar\beta$, as illustrated in Fig. 4(a).

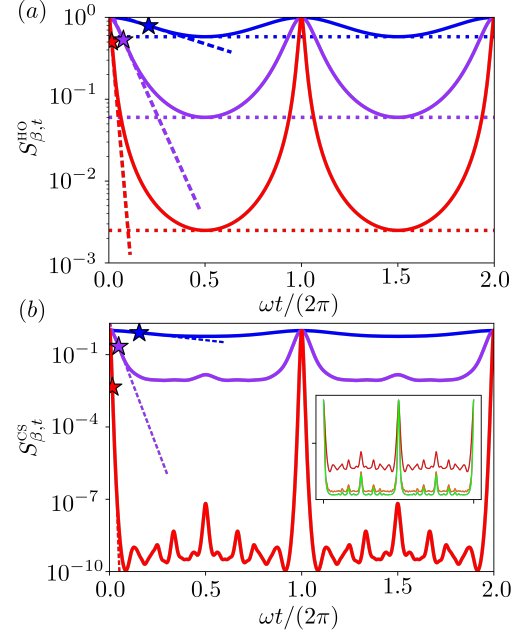


Figure 3: **Time evolution of the spectral form factor** for the (a) harmonic oscillator (15) and (b) Calogero-Sutherland model (18) at $\beta\hbar\omega = 2$ (blue), 0.5 (purple) and 0.1 (red). The dashed lines represent the function $e^{-\eta t}$ around the inflection time t_0 , marked by a star. (a) The dotted lines mark the SFF minimum values. (b) SFF for $N = 10$. The inset shows the SFF evolution at $\beta\hbar\omega = 0.1$ for $N = 10$ (red), 30 (dashed orange) and 100 (solid green) interacting particles—the two red curves coincide. Increasing the temperature or the number of particles makes the SFF reach lower values.

3.2 Many-body integrable system: the Calogero-Sutherland model

The Calogero-Sutherland (CS) model is a many-body system of N particles in one dimension with inverse-square interactions [67, 68] that gives insight into black-hole physics [69–71]. The Hamiltonian reads, in first quantization,

$$\hat{H} = \sum_{n=1}^N \left(-\frac{1}{2} \frac{\partial^2}{\partial x_n^2} + \frac{1}{2} \omega^2 x_n^2 \right) + \sum_{n < n'} \frac{\ell(\ell-1)}{(x_n - x_{n'})^2}, \quad (17)$$

where ℓ determines the interaction strength and ω is the frequency of the harmonic trap in which the particles are confined. This model is equivalent to an ideal gas of Haldane anyons [72, 73], so its partition function factorizes—as expected for an ideal gas [74]. This factorization leads to the SFF being the product of the SFF for N harmonic oscillators (15) with increasing frequencies

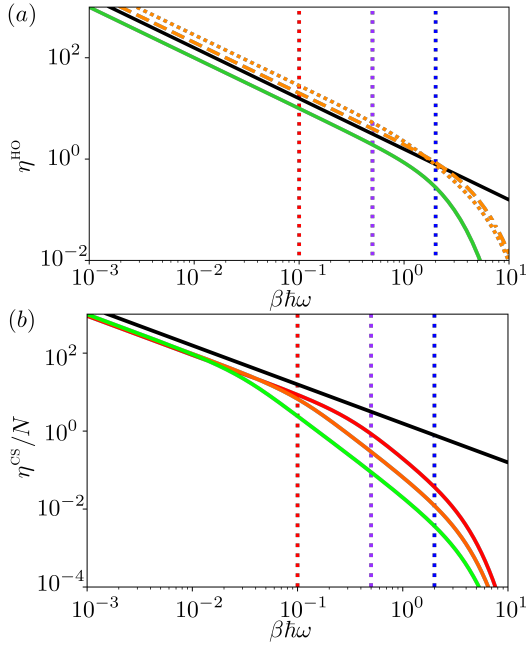


Figure 4: **Inflection exponent** and its bound (9) (black line) as function of the dimension-less inverse temperature $\beta\hbar\omega$ for the (a) harmonic oscillator η (green) and (b) Calogero-Sutherland model η_β^{CS}/N for $N = 10$ (red), 30 (dashed orange) and 100 (green). The vertical dotted lines represent the inverse temperatures shown in Fig. 3. (a) The orange lines show bounds from QSL η_{QSL} (27) (dotted line) and from the Bhattacharyya results η_{B} (28) (dashed line).

$n\omega$, namely [17, 75]

$$S_{\beta,t}^{\text{CS}} = \prod_{n=1}^N \frac{\cosh(n\hbar\omega\beta) - 1}{\cosh(n\hbar\omega\beta) - \cos(n\omega t)}. \quad (18)$$

Note that this simple result does not hold when the trap frequency is time dependent [76]. The behavior of this SFF is illustrated in Fig. 3(b): it is also $2\pi/\omega$ periodic but shows higher order peaks corresponding to the ‘harmonics’ $n\omega$, particularly apparent for $n = 2$ and $n = 3$. Increasing the temperature $1/\beta$ or the number of particles N (see inset) makes the SFF reach lower values.

The inflection exponent easily follows from $\ln S_{\beta,t}^{\text{CS}} = \sum_n \ln S_{\beta,t}^{\text{HO}}(n\omega)$ as

$$\eta_\beta^{\text{CS}} = \sum_n \eta_\beta^{\text{HO}}(n\omega) = \sum_{n=1}^N \frac{n\omega}{\sinh(n\beta\hbar\omega)}. \quad (19)$$

Its dependence with the inverse temperature is shown in Fig. 4(b). To compare it with the bound, we use the intensive quantity η^{CS}/N , as conjectured in (10). The many-body interaction effectively leads to two main regimes: one

at very high temperatures in which the behavior is similar to a single harmonic oscillator, *i.e.* $\eta^{\text{CS}}/N \sim \beta^{-1}$, and one at intermediate temperatures in which η^{CS}/N decays faster. This region grows with the number of interacting particles N .

3.3 Chaotic dynamics: random matrix ensemble

We now look at a typical chaotic system chosen within the common playground of random matrix theory [17, 57–59, 77–80]. A Hermitian system with independent matrix elements and no time-reversal symmetry is represented by the Gaussian Unitary Ensemble (GUE) [59]. Averaging over a random matrix ensemble yields eigenenergies which are correlated in the same way as in a quantum chaotic system, according to the *Bohigas-Giannoni-Schmit conjecture* [81, 82]. A constituent of the ensemble is constructed by sampling every matrix element from a Gaussian distribution with standard deviation $\sigma = \hbar\omega_{\text{GUE}}$. For the diagonal elements the Gaussian is real and for the off-diagonal it is complex, therefore the constructed Hamiltonian will be Hermitian. The ensemble averaging of the SFF (1) should rigorously be taken such that $\left\langle \frac{|Z_{\beta+it/\hbar}|^2}{Z_\beta^2} \right\rangle$ to represent physically measurable quantities, but the ‘annealed’ version, with the average split as $\frac{\langle |Z_{\beta+it/\hbar}|^2 \rangle}{\langle Z_\beta^2 \rangle}$, is useful to obtain analytical results. Both averages are equal in the high-temperature limit. In the context of random matrix theory, the ensemble averaged SFF is commonly split into three terms,

$$S_{\beta,t}^{\text{GUE}} = \frac{\langle Z_{2\beta} \rangle + |\langle Z_{\beta+it/\hbar} \rangle|^2 + g_c(\beta, t)}{\langle Z_\beta \rangle^2}, \quad (20)$$

where the connected SFF $g_c(\beta, t)$ is detailed in App. B. The averaged partition function for the GUE in a \mathcal{N} -dimensional Hilbert space is known as [17]

$$\langle Z_{\beta+it/\hbar} \rangle = e^{\frac{(\beta+it/\hbar)^2}{4}} L_{\mathcal{N}-1}^1 \left(-\frac{(\beta+it/\hbar)^2}{2} \right), \quad (21)$$

where $L_n^\alpha(x) = \sum_{j=0}^n \binom{n+\alpha}{n-j} \frac{(-x)^j}{j!}$ are the generalized Laguerre polynomials.

Figure 5(a) shows the SFF computed numerically and analytically for the GUE. The behavior displays the shape (slope-dip-ramp-plateau) characteristic of chaotic systems. As the system

temperature is decreased, the dip becomes shallower and occurs later. This is because the SFF accounts for all the possible energy correlations across the full spectrum: as the temperature is lowered, the contributions from neighbors further apart in energy—that have a smaller dip time—decreases, such that the dip time is delayed. This behavior is explicit from an expression of the SFF as function of the energy neighbors that we give in App. B.

The function $e^{-\eta t}$ around the inflection point is also shown in Fig. 5(a). The dependence of the η exponent as a function of the inverse system temperature is shown in Fig. 6(a), together with its bound. We see that the exponent gets close to the bound (9) for $0.1 \lesssim \beta \hbar \omega_{\text{GUE}} \lesssim 1$. Interestingly, the exponent saturates to a constant value at high temperature, a feature not present in the harmonic oscillator, that is related to the finiteness of the Hilbert space \mathcal{N} : beyond some high enough temperature, all energy levels are already included within the thermal average and the saturation happens.

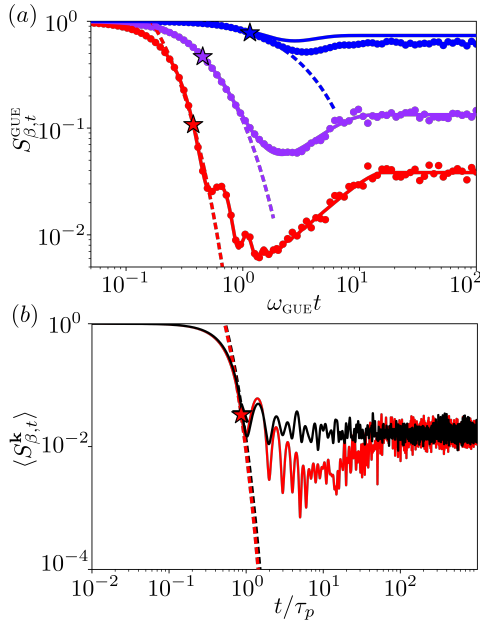


Figure 5: **Time evolution of the SFF** for (a) the Gaussian Unitary Ensemble of dimension $\mathcal{N} = 30$ and (b) the quantum kicked top. The dashed lines represent the function $e^{-\eta t}$ around the inflection time t_0 , marked by a star. (a) The dots represent the numerical average over $N_{\text{av}} = 100$ realizations, the solid lines represent the ‘annealed’ analytical expression (20) for $\hbar\beta = 2$ (blue), 0.5 (purple) and 0.1 (red). (b) SFF for the quantum kicked top (24) in the regular (black) and chaotic (red) regime, at $\hbar\beta = 0.1$, with spin $S = 30$ and a numerical average over $N_{\text{av}} = 30$ realizations.

3.4 Tunable dynamics: generalized quantum kicked top

We now look at a system which dynamics can be tuned from regular to chaotic motion, the quantum kicked top, which was designed in the early days of quantum chaos studies and remains an important playground [43, 60, 83–88]. Kicked tops model a spin S system subject to a free precession and some τ_p periodic kicks, the strength of which allows going from periodic orbits to chaotic dynamics. The stroboscopic description of such a periodic system is well characterized in terms of the Floquet operator, which captures the time evolution of the system over one period.

We use the Floquet operator for the general unitary class introduced by Haake [88]

$$\hat{U} = e^{-i(\frac{p_z}{\hbar}\hat{S}_z + \frac{1}{(2S+1)\hbar^2}k_z\hat{S}_z^2)} e^{-i(\frac{p_y}{\hbar}\hat{S}_y + \frac{1}{(2S+1)\hbar^2}k_y\hat{S}_y^2)} \times e^{-i(\frac{p_x}{\hbar}\hat{S}_x + \frac{1}{(2S+1)\hbar^2}k_x\hat{S}_x^2)}, \quad (22)$$

that can mimic the behavior of any members of a universality class displayed by random matrix theory according to the choice of parameters $\mathbf{p} = (p_x, p_y, p_z)$ and $\mathbf{k} = (k_x, k_y, k_z)$, where $\hat{\mathbf{S}} = (\hat{S}_x, \hat{S}_y, \hat{S}_z)$ are the general spin operators. For example, for $\mathbf{k} \times \mathbf{p} = 0$, e.g. the only non-zero terms are $k_z = 1$ and $p_z = 10$, the system is integrable (the level spacings follow Poisson statistics) because of the extra symmetry $[\hat{U}, \hat{S}_z] = 0$ that brings an extra conserved quantity—the z -component of the angular momentum. There are choices of parameters that break time-reversal symmetry and therefore the system behaves similarly to the GUE, e.g. $\mathbf{p} = (1.1, 1, 1)$ and $\mathbf{k} = (4, 0, 10)$.

The eigenvalues of the Floquet operator, $\hat{U}|\chi_j\rangle = e^{-i\omega_j^{\mathbf{k}}\tau_p}|\chi_j\rangle$, allow defining the pseudo-frequencies $\omega_j^{\mathbf{k}}$ [89, 90]. For our purpose, we use these pseudo-frequencies to define the pseudo-SFF as

$$S_{\beta,t}^{\mathbf{k}} = \frac{\sum_{m,n} e^{-(\beta\hbar + it)\omega_m^{\mathbf{k}}} e^{-(\beta\hbar - it)\omega_n^{\mathbf{k}}}}{\left(\sum_m e^{-\beta\hbar\omega_m^{\mathbf{k}}}\right)^2}. \quad (23)$$

The SFF is in general not a self-averaging quantity [66], which means its behavior over one system realization generally differs from the ensemble average. To obtain an average behavior, we follow Haake’s original idea [60] and introduce an averaging over some window of parameters. We uniformly generate N_{av} random points in the

interval $\mathcal{K} \equiv (k_z - \delta k_z/2, k_z + \delta k_z/2)$ and average over them to obtain

$$\langle S_{\beta,t}^{\mathbf{k}} \rangle = \frac{1}{N_{\text{av}}} \sum_{\kappa \in \mathcal{K}} S_{\beta,t}^{(k_x, k_y, \kappa)}, \quad (24)$$

where we choose $\delta k_z = 0.05 k_z$. Fig. 5(b) shows the pseudo-SFF computed for the kicked top in the two dynamical regimes, regular and chaotic. In the latter, $\langle S_{\beta,t}^{\mathbf{k}} \rangle$ exhibits the expected behavior in the chaotic phase, with a dip and a ramp at long times, absent in the former. Around the t_0 inflection point, both regimes behave quite similarly. This holds over a wide range of temperatures, as illustrated by the inflection exponent η behavior in Fig. 6(b). In both regimes, the exponent gets very close to the bound (9) imposed by analyticity, therefore the tightness of the bound is not related to regular or chaotic dynamics. The saturation at high temperatures observed in the GUE is also present here because the kicked top has a finite dimensional Hilbert space, with $\mathcal{N} = 2S + 1$.

4 Relation to quantum speed limits and other known bounds

We explore below the relation of the derived bound with other known bounds.

Quantum Speed Limits (QSL) set a bound on the evolution of the fidelity. For a pure state under unitary dynamics, the rate of change of the fidelity $F_t = |\langle \psi_t | \psi_0 \rangle|^2$ is bounded by [11]

$$|\dot{F}_t| \leq \frac{\sqrt{2}}{\hbar} \Delta E, \quad (25)$$

where $\Delta E = \sqrt{\langle H^2 \rangle - \langle H \rangle^2}$ captures the energy fluctuations. Since the SFF is the fidelity of the pure, coherent Gibbs state, this bound applies to $S_{\beta,t}$ defined in Eq. (1). In order to compare this bound with that on the inflection exponent (9), we look at the inequality obtained from QSL at time t_0 , that yields

$$\eta = \frac{|\dot{S}_{\beta,t_0}|}{S_{\beta,t_0}} \leq \eta_{\text{QSL}} \equiv \frac{\sqrt{2}}{\hbar} \frac{\Delta E}{S_{\beta,t_0}}. \quad (26)$$

For the example of the harmonic oscillator considered above, we easily get (see App. C for details)

$$\begin{aligned} |\dot{S}_{\beta,t}^{\text{HO}}| &= \frac{|\omega \sin(\omega t)(1 - \cosh(\beta \hbar \omega))|}{(\cosh(\beta \hbar \omega) - \cos(\omega t))^2} \\ &\leq \frac{\sqrt{2}}{\hbar} \Delta E = \sqrt{2} \omega Z_\beta, \end{aligned} \quad (27)$$

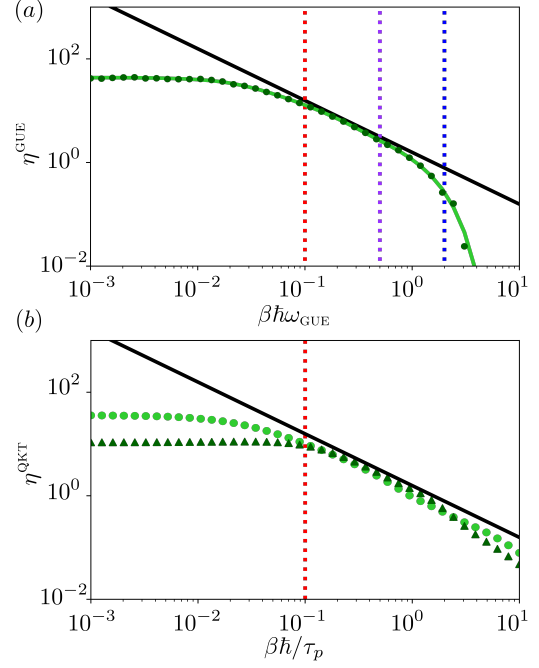


Figure 6: **Inflection exponent** η (green) and its bound (Eq. (9), black line) as function of the inverse temperature β for (a) the Gaussian Unitary Ensemble and (b) the quantum kicked top. The vertical dotted lines represent the inverse temperatures shown in Fig. 5. Results in the quantum kicked top (b) are shown for the two dynamical regimes illustrated in Fig. 5(b), chaotic (green circles) and regular (dark green triangles). The inflection exponent η^{QKT} gets close to the analyticity bound for $0.2 \lesssim \beta \hbar \lesssim 2$ in both dynamical regimes, which further confirms the independence of η on the dynamics of the system.

which further yields $\eta \leq \sqrt{2} \omega Z_\beta [\cosh(\beta \hbar \omega) + 1] / \cosh(\beta \hbar \omega)$. Fig. 4(a) shows that the universal bound imposed by analyticity (9) is tighter than that imposed by QSL for temperatures above $\beta \hbar \omega \approx 2$. The asymptotic value of the QSL at high temperatures is $2\sqrt{2}/(\beta \hbar)$.

Also note that the survival probability, when larger than $1/2$, can be lower bounded by an exponential function, as shown by Bhattacharyya [91]. This result has been extended to the spectral form factor [17] and reads $S_{\beta,t} \geq e^{-2\Delta E t/\hbar}$. This lower bound gives an upper bound on the inflection exponent, namely

$$\eta \leq \eta_B = \frac{2}{\hbar} \Delta E. \quad (28)$$

For the harmonic oscillator, it is $\eta_B^{\text{HO}} = 2\omega Z_\beta$. Fig. 4(a) compares all three bounds for the harmonic oscillator, in which system the universal bound set by analyticity constraints is the tightest at high enough temperature ($\beta \hbar \omega \lesssim 2$).

Bounds defined from the temperature and the Planck constant only, so-called Planckian bounds, have raised a renewed interest [50, 51, 92]. The bound on the Lyapunov exponent has thus been related to the fluctuation-dissipation theorem in the time domain [51]. Specifically, the OTOC corresponds to a two-point correlation function in a doubled Hilbert space, where the out-of-time ordering is introduced by a swap operator between the two Hilbert spaces. The two-point correlation function $\frac{1}{Z_\beta} \text{Tr}(e^{-\beta \hat{H}} \hat{A}_t \hat{B})$ can be split as $C_{AB}(t) + \hbar R''_{AB}(t) = \frac{1}{2Z_\beta} \text{Tr}(e^{-\beta \hat{H}} \{\hat{A}_t, \hat{B}\}) + \frac{1}{2Z_\beta} \text{Tr}(e^{-\beta \hat{H}} [\hat{A}_t, \hat{B}])$, that is, into terms characterizing fluctuations and the response to external perturbations, respectively. The regulated form of this correlator,

$$\mathcal{F}_{AB}(\beta, t) = \frac{1}{Z_\beta} \text{Tr}(e^{-\frac{\beta}{2} \hat{H}} \hat{A}_t e^{-\frac{\beta}{2} \hat{H}} \hat{B}), \quad (29)$$

is similar to an OTOC when going to a doubled Hilbert space and introducing a swap operator. By using the fluctuation-dissipation theorem, the authors in [51] find a Planckian bound on two-point correlators, thus connecting with the MSS finding. Specifically, if the fluctuation term $C(t)$ decays exponentially, then $\mathcal{F}(t)$ decays exponentially as $\mathcal{F}(t) \sim e^{-t/\tau}$, with a rate bounded by $\frac{1}{\tau} \leq \frac{\pi}{\beta \hbar}$. This bound is actually also related to the one we derive, since, for $A_{m,n} = \frac{Z_\beta^{1/2}}{Z_{\beta/2}} \forall(m, n)$, the regulated two-point correlator corresponds to the SFF at double the temperature, $\mathcal{F}_{AA}(\beta, t) \equiv S_{\beta/2, t}$. We then have $\eta \leq \frac{\pi}{\beta \hbar}$, which matches our bound under the substitution $\beta \rightarrow \beta/2$ in (9). The main difference between the two approaches is that two-point correlation functions are not analytic at $t = 0$ while we have shown that the SFF is analytic at $t = 0$.

The work [93] finds bounds on transport coefficients through analyticity properties. The author uses univalence, the property of a complex function of being injective, and by finding domains in which the functions are univalent one can find bounds on physical properties like transport coefficients in hydrodynamic theories.

5 Conclusion

We introduced the *inflection exponent* η to characterize the early-time decay of the SFF, that happens after the initial Gaussian decay and we

find can be approximated by an exponential. This exponent is related to the imaginary part of the average energy at complex temperature. Following arguments from complex analysis, we have found that it is bounded as $\eta \leq \pi/(2\beta \hbar)$. By contrast with the MSS bound on chaos, which is only saturated by black holes [25] and their holographic duals, like the Sachdev-Ye-Kitaev model [31], our bound on the SFF is already quite tight in a variety of systems.

We illustrated the bound in systems representing regular and chaotic dynamics. At high temperature, the behavior of the exponent depends on whether the system Hilbert space is infinite dimensional or not. Indeed, this determines if more energy levels become available as the temperature increases, or not, in which later case the exponent saturates at a fixed value. Importantly, the behavior of η is similar in the GUE and the quantum kicked top, even if the latter is tuned in the regular regime.

Our results, based on analyticity constraints, set a bound on the fidelity of the coherent Gibbs state. We show how they relate to known results from quantum speed limits, that set a bound on the fidelity based on unitary dynamics. Further investigation in this direction would look for possible extension of the bound set by the domain of analyticity to other dynamical quantities and even different domains of analyticity, which may change the functional dependence of the quantities that can be bounded.

Acknowledgements

It is a pleasure to thank A. del Campo, J. Yang, A. Kundu, J. Pomar, S. Pappalardi, F. Roccati and R. Shir for insightful discussions and B. Mukhametzhanov and F. Balducci for comments on the manuscript. AC thanks the hospitality of the DIPC during revision of the manuscript. This work was partially funded by the Luxembourg National Research Fund (FNR, Attract grant 15382998) and by the John Templeton Foundation (Grant 62171). The opinions expressed in this publication are those of the authors and do not necessarily reflect the views of the John Templeton Foundation.

A Analyticity of the Spectral Form Factor

We show below that the analytical continuation of the SFF, $S_{\beta,t+i\tau}$, is analytic in the strip $-\beta\hbar \leq \tau \leq +\beta\hbar$ and $t \in \mathbb{R}$.

A function of complex variable $f(x + iy) = u(x, y) + iv(x, y)$ is analytic at $z_0 = x_0 + iy_0$ if and only if it is holomorphic, i.e. complex differentiable, at this point. For $f(z)$ to be holomorphic it has to obey the Cauchy-Riemann conditions at this point, $\partial_x u = \partial_y v$ and $\partial_y u = -\partial_x v$, and the partial derivatives $\partial_x u, \partial_y u, \partial_x v, \partial_y v$ have to be continuous at z_0 . The SFF at complex time, defined in Eq. (3), can be written as

$$\begin{aligned} S_{\beta,t+i\tau} &= \sum_m \frac{e^{-2\beta E_m}}{Z_\beta^2} + \sum_{m \neq n} \frac{e^{-\beta \bar{E}_{mn} + \tau \omega_{mn}}}{Z_\beta^2} \cos(\omega_{mn} t) \\ &\quad - i \sum_{m \neq n} \frac{e^{-\beta \bar{E}_{mn} + \tau \omega_{mn}}}{Z_\beta^2} \sin(\omega_{mn} t), \quad (\text{S1}) \\ &\equiv u(t, \tau) + iv(t, \tau) \end{aligned}$$

where we introduced $\bar{E}_{mn} = E_m + E_n$ and $\omega_{mn} = (E_m - E_n)/\hbar$. The partial derivatives then read

$$\begin{aligned} \partial_t u &= - \sum_{m \neq n} \frac{\omega_{mn}}{Z_\beta^2} e^{-\beta \bar{E}_{mn} + \tau \omega_{mn}} \sin(\omega_{mn} t) = \partial_\tau v, \\ \partial_\tau u &= \sum_{m \neq n} \frac{\omega_{mn}}{Z_\beta^2} e^{-\beta \bar{E}_{mn} + \tau \omega_{mn}} \cos(\omega_{mn} t) = -\partial_t v. \end{aligned}$$

So the Cauchy-Riemann conditions are satisfied.

Let us now check if, for an infinite dimensional Hilbert space, the sums appearing in the definition of the SFF and its derivatives converge. To do so, we use the *ratio test*: given a series of the form $\sum_{n=0}^{\infty} a_n$, the ratio test is based on the value of the limit

$$L = \lim_{n \rightarrow \infty} \left| \frac{a_{n+1}}{a_n} \right|.$$

If $L < 1$, the sum *absolutely* converges, if $L > 1$ the sum diverges, and if $L = 1$ the test is inconclusive. Recall that absolute convergence means $\sum_n |a_n| = L$.

To check the convergence of the SFF

$$S_{\beta,t+i\tau} = \frac{1}{Z_\beta^2} \sum_{m=0}^{\infty} e^{-(\beta - \frac{\tau}{\hbar} + i\frac{t}{\hbar})E_m} \sum_{n=0}^{\infty} e^{-(\beta + \frac{\tau}{\hbar} - i\frac{t}{\hbar})E_n},$$

we split the double sum into the product of two sums. This is true if at least one of the sum

absolutely converges—*Mertens' theorem* on the Cauchy product. We thus look at the limit of each sum, that we denote L_1 and L_2 . Considering that the energies are ordered $E_{m+1} \geq E_m$ and assuming no degeneracies at infinity, the test yields the following limits

$$\begin{aligned} L_1 &= \lim_{m \rightarrow \infty} e^{-(\beta - \frac{\tau}{\hbar})(E_{m+1} - E_m)} < 1 \quad \text{if } \beta - \frac{\tau}{\hbar} > 0, \\ L_2 &= \lim_{n \rightarrow \infty} e^{-(\beta + \frac{\tau}{\hbar})(E_{n+1} - E_n)} < 1 \quad \text{if } \beta + \frac{\tau}{\hbar} > 0. \end{aligned}$$

So, the SFF converges within the region $-\beta < \frac{\tau}{\hbar} < \beta$. In addition, the ‘effective inverse temperature’ $\beta \pm \frac{\tau}{\hbar}$ is positive and the partition function also converges.

Now, to check that the sums in the partial derivatives of the SFF also converge, we study the convergence of

$$\sum_{m,n} (E_m - E_n) e^{-(\beta - \frac{\tau}{\hbar} + i\frac{t}{\hbar})E_m} e^{-(\beta + \frac{\tau}{\hbar} - i\frac{t}{\hbar})E_n}.$$

We thus have to check the convergence of two sums of the form

$$\sum_m E_m e^{-(\beta \mp \frac{\tau}{\hbar} + i\frac{t}{\hbar})E_m} \sum_n e^{-(\beta \pm \frac{\tau}{\hbar} - i\frac{t}{\hbar})E_n}.$$

The second sum was already shown to converge. The ratio test for the first sum gives

$$L = \lim_{m \rightarrow \infty} \left| \frac{E_{m+1}}{E_m} e^{-(\beta \mp \frac{\tau}{\hbar} + i\frac{t}{\hbar})(E_{m+1} - E_m)} \right|.$$

Introducing the dimensionless level-spacing $s_m = \frac{E_{m+1} - E_m}{E_m}$, the limit can be rewritten as

$$L = \lim_{m \rightarrow \infty} (1 + s_m) e^{-(\beta \mp \frac{\tau}{\hbar})E_m s_m}.$$

Now, the function $f(x) = (1 + x)e^{-ax}$ is smaller than one $\forall x > 0$ if $a > 1$. So the two series converge provided that

$$(\beta - \frac{\tau}{\hbar})E_m > 1 \rightarrow \tau < \beta\hbar - \lim_{m \rightarrow \infty} \left(\frac{\hbar}{E_m} \right),$$

$$(\beta + \frac{\tau}{\hbar})E_m > 1 \rightarrow \tau > -\beta\hbar + \lim_{m \rightarrow \infty} \left(\frac{\hbar}{E_m} \right).$$

Assuming that the spectrum is unbounded, i.e. $E_m \rightarrow \infty$ for $m \rightarrow \infty$, we get the same strip $-\beta\hbar < \tau < \beta\hbar$. This verifies that the SFF is analytic in the strip $-\beta\hbar \leq \tau \leq +\beta\hbar$, including at $t = 0$.

B Spectral form factor in the Gaussian Unitary Ensemble

B.1 Connected SFF

We first detail the connected SFF,

$$g_c(\beta, t) = \int dE dE' \langle \rho_c^{(2)}(E, E') \rangle e^{-(\beta + \frac{it}{\hbar})E - (\beta - \frac{it}{\hbar})E'}, \quad (\text{S2})$$

that is the double complex Fourier transform of the connected correlation function $\langle \rho_c^{(2)}(E, E') \rangle = \langle \rho(E) \rho(E') \rangle - \langle \rho(E) \rangle \langle \rho(E') \rangle$, where $\langle \rho(E) \rangle$ is the density of states and $\langle \rho(E) \rho(E') \rangle$ is the 2-level correlation function which gives the probability density of finding a level around E and another one around E' [59]. An analytical expression is known for the GUE, and reads [80]

$$g_c(\sigma, \sigma^*) = -e^{\frac{\sigma^2 + \sigma^{*2}}{4}} \sum_{n,m=0}^{\mathcal{N}-1} \frac{\min(m, n)!}{\max(m, n)!} \times \left(\frac{|\sigma|^2}{2} \right)^{|n-m|} \left| L_{\min(m, n)}^{|n-m|} \left(-\frac{\sigma^2}{2} \right) \right|^2, \quad (\text{S3})$$

with the complex value $\sigma = \beta + \frac{it}{\hbar}$.

B.2 Influence of the system size \mathcal{N}

Then, we look at the influence that the system size \mathcal{N} has on the inflection exponent η . Fig. 7 illustrates the role of large \mathcal{N} in the region in which we get close to the bound imposed by analyticity, Eq. (9) in the main text. This region is observed to grow with the system size. Indeed for very low-dimensional Hilbert spaces, e.g. $\mathcal{N} = 2$, the inflection exponent does not get close to the bound. The saturation value of the inflection exponent $\lim_{\beta \rightarrow 0} \eta$ at high temperatures is also seen to grow with the system size.

B.3 SFF as function of the neighbor rank

From the definition of the SFF,

$$S_{\beta, t} = \frac{1}{Z_\beta^2} \sum_{n, m=1}^{\mathcal{N}} e^{-\beta(E_m + E_n)} e^{-\frac{it}{\hbar}(E_n - E_m)}, \quad (\text{S4})$$

it is clear that this quantity carries information from all correlations across the full spectrum and not just those from nearest energy neighbors, which are captured by the nearest-neighbor level spacing. These energy correlations are associated

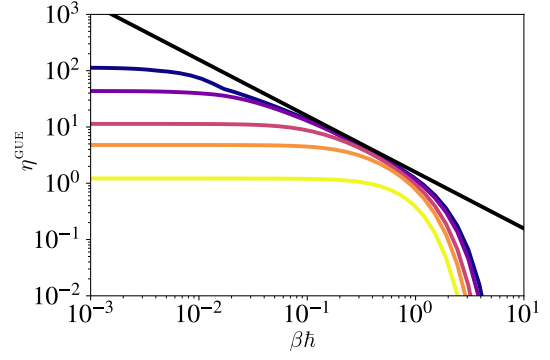


Figure 7: **Scaling of the inflection exponent** η for the Gaussian Unitary Ensemble as a function of the inverse temperature β for different system size: $\mathcal{N} = 2$ (yellow), 5 (orange), 10 (pink), 30 (purple) and 50 (blue). Results are computed numerically from the analytical expression of the SFF for the GUE, Eq. (20). The black line represents the bound imposed by analyticity, Eq. (9) in the main text.

with chaotic behavior and give rise to the ramp, as discussed in the main text.

The SFF may be written such as to make the role of the energy correlations explicit. For this, we introduce the j -th level spacing $s_n^{(j)}$ as the difference between j -th neighboring energies, namely $s_n^{(j)} = E_{n+j} - E_n$. The SFF becomes

$$S_{\beta, t} = \frac{Z_{2\beta}}{Z_\beta^2} + \sum_{j=1}^{\mathcal{N}-1} S_{\beta, t}^{(j)}, \quad (\text{S5})$$

where $S_{\beta, t}^{(j)}$ is the contribution of the j -th energy neighbors, defined as

$$S_{\beta, t}^{(j)} = \frac{2}{Z_\beta^2} \sum_{n=0}^{\mathcal{N}-j} \cos\left(\frac{s_n^{(j)} t}{\hbar}\right) e^{-\beta(2E_n + s_n^{(j)})}. \quad (\text{S6})$$

Figure 8 shows the contributions of the different neighbor rank j to the SFF. We see how the further away the energies are, that is, the larger the rank j , the sooner the dip time. This behavior is not surprising because for larger energy difference $s_n^{(j)}$, the time required to explore the full Hilbert space is shorter. At infinite temperature, Fig. 8(a) shows that the contribution at short times is larger for neighbors of lower rank, i.e. energies closer together. The role of finite temperature can be understood from Fig. 8(b), where the contributions for neighbors further apart, i.e. larger j , vanish with the term $e^{-\beta s_n^{(j)}}$ in (S6). This explains why the dip time is delayed as the system temperature decreases, i.e.

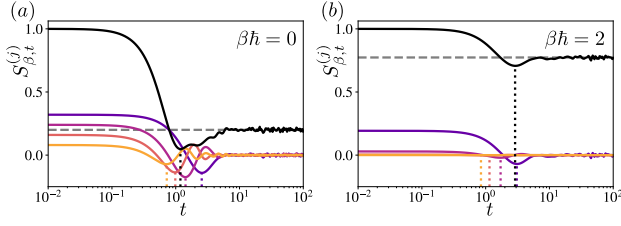


Figure 8: **Contributions from j -th neighbors $S_{\beta,t}^{(j)}$ to the spectral form factor $S_{\beta,t}$** (exact average) for the Gaussian Unitary Ensemble computed numerically at two different inverse temperatures (a) $\beta\hbar = 0$ and (b) $\beta\hbar = 2$. The full SFF $S_{\beta,t}$ (solid black line), reaches the plateau $\langle Z_{2\beta}/Z_{\beta}^2 \rangle$ (grey dashed line) at large time. The contributions $S_{\beta,t}^{(j)}$, as defined in (S6), are shown for $j = 1$ (purple), 2 (pink), 3 (red) and 4 (orange). The dotted lines mark the dip time of each contribution $S_{\beta,t}^{(j)}$. Here, $\mathcal{N} = 5$ for clarity of the plot and the results are averaged over $N_{\text{av}} = 300$ realizations of the GUE.

because the contributions for neighbors further apart in energy progressively vanish. This also shows how, at low temperatures, the SFF may be approximated from the contribution of nearest-neighbors $S_{\beta,t}^{(1)}$. This is reasonable since, as the temperature is lowered, the levels correlate less with levels further apart, and the most relevant contribution is captured by nearest-neighbors in energy.

C Quantum Speed Limits on the SFF for the Harmonic Oscillator

Quantum Speed Limits set a bound on the time derivative of the fidelity of pure states given by [11]

$$|\dot{F}_t| \leq \frac{\sqrt{2}}{\hbar} \Delta E. \quad (\text{S7})$$

The SFF may be interpreted as the fidelity between the coherent Gibbs state $|\psi_{\beta}\rangle$ and its time evolution, so the QSL on the fidelity yields a QSL on the SFF. The standard deviation of the energy thus needs to be taken with respect to the coherent Gibbs states, which mimic thermal averages, i.e. $\langle \psi_{\beta} | \hat{H}^n | \psi_{\beta} \rangle = \text{Tr}(\hat{H}^n e^{-\beta \hat{H}}) / Z_{\beta} = (-1)^n Z_{\beta}^{-1} d^n Z_{\beta} / d\beta^n$. The first two thermal mo-

ments,

$$\begin{aligned} \langle \hat{H} \rangle &= -\frac{1}{Z_{\beta}} \frac{dZ_{\beta}}{d\beta} = \frac{\hbar\omega}{2} \coth \frac{\beta\hbar\omega}{2}, \\ \langle \hat{H}^2 \rangle &= \frac{1}{Z_{\beta}} \frac{d^2 Z_{\beta}}{d\beta^2} = \frac{(\hbar\omega)^2}{4} \left(2 \coth^2 \frac{\beta\hbar\omega}{2} - 1 \right), \end{aligned} \quad (\text{S8})$$

yield the standard deviation of the energy $\Delta E = \sqrt{\langle H^2 \rangle - \langle H \rangle^2}$ as

$$\Delta E = \frac{\hbar\omega}{2} \sqrt{\coth^2 \frac{\beta\hbar\omega}{2} - 1} = \frac{\hbar\omega}{2 \sinh \frac{\beta\hbar\omega}{2}} \quad (\text{S9})$$

which simplifies to $\hbar\omega Z_{\beta}$.

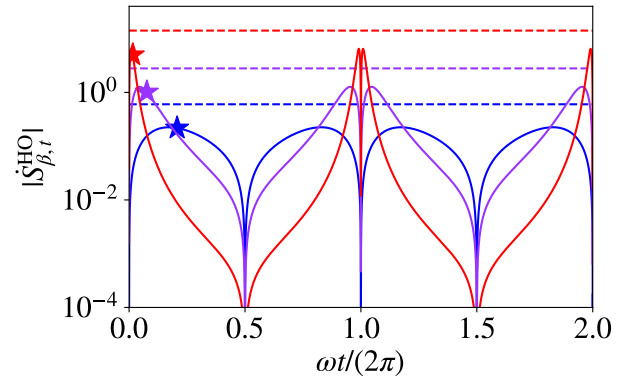


Figure 9: **Quantum Speed Limit** on the SFF for the harmonic oscillator at inverse temperatures $\beta = 2$ (blue), 0.5 (purple) and 0.1 (red). The solid lines represent $|\dot{S}_{\beta,t}^{\text{HO}}|$, eq. (16) in the main text, bounded by the QSL on fidelity (S7) (dashed lines), obtained with the energy standard deviation of Eq. (S9). The stars represent the inflection point of $\ln(S_{\beta,t}^{\text{HO}})$.

Figure 9 shows the time derivative of the SFF together with the bound set by the QSL on the fidelity (S7). This bound increases with the temperature, in a fashion similar to the maximum value of $|\dot{S}_{\beta,t}^{\text{HO}}|$. The inflection point of $\ln(S_{\beta,t}^{\text{HO}})$ is close to the maximum of $|\dot{S}_{\beta,t}^{\text{HO}}|$ which corresponds to the inflection point of $S_{\beta,t}^{\text{HO}}$.

References

- [1] L. Mandelstam and I. Tamm, in *Selected Papers*, edited by I. E. Tamm, B. M. Boltovskii, V. Y. Frenkel, and R. Peierls (Springer, Berlin, Heidelberg, 1991) pp. 115–123.
- [2] N. Margolus and L. B. Levitin, *Physica D: Nonlinear Phenomena Proceedings of the*

- [3] L. B. Levitin and T. Toffoli, *Phys. Rev. Lett.* **103**, 160502 (2009).
- [4] A. del Campo, I. L. Egusquiza, M. B. Plenio, and S. F. Huelga, *Phys. Rev. Lett.* **110**, 050403 (2013).
- [5] M. M. Taddei, B. M. Escher, L. Davidovich, and R. L. de Matos Filho, *Phys. Rev. Lett.* **110**, 050402 (2013).
- [6] P. Pfeifer and J. Fröhlich, *Rev. Mod. Phys.* **67**, 759 (1995).
- [7] G. Muga, R. S. Mayato, and I. Egusquiza, eds., *Time in Quantum Mechanics*, 2nd ed., Lecture Notes in Physics (Springer-Verlag, Berlin Heidelberg, 2008).
- [8] G. Muga, A. Ruschhaupt, and A. Campo, *Time in Quantum Mechanics-Vol. 2*, Vol. 789 (2009).
- [9] M. R. Frey, *Quantum Inf Process* **15**, 3919 (2016).
- [10] S. Deffner and S. Campbell, *J. Phys. A: Math. Theor.* **50**, 453001 (2017).
- [11] B. Shanahan, A. Chenu, N. Margolus, and A. del Campo, *Phys. Rev. Lett.* **120**, 070401 (2018).
- [12] M. Okuyama and M. Ohzeki, *Phys. Rev. Lett.* **120**, 070402 (2018).
- [13] P. M. Poggi, S. Campbell, and S. Deffner, *PRX Quantum* **2**, 040349 (2021).
- [14] L. P. García-Pintos, S. B. Nicholson, J. R. Green, A. del Campo, and A. V. Gorshkov, *Physical Review X* **12**, 011038 (2022).
- [15] J. D. Bekenstein, *Phys. Rev. Lett.* **46**, 623 (1981).
- [16] S. Lloyd, *Nature* **406**, 1047 (2000).
- [17] A. del Campo, J. Molina-Vilaplana, and J. Sonner, *Phys. Rev. D* **95**, 126008 (2017).
- [18] M. Bukov, D. Sels, and A. Polkovnikov, *Physical Review X* **9**, 011034 (2019).
- [19] T. Fogarty, S. Deffner, T. Busch, and S. Campbell, *Physical Review Letters* **124**, 110601 (2020).
- [20] A. del Campo, *Physical Review Letters* **126**, 180603 (2021).
- [21] T. Caneva, M. Murphy, T. Calarco, R. Fazio, S. Montangero, V. Giovannetti, and G. E. Santoro, *Phys. Rev. Lett.* **103**, 240501 (2009).
- [22] K. Funo, J.-N. Zhang, C. Chatou, K. Kim, M. Ueda, and A. del Campo, *Phys. Rev. Lett.* **118**, 100602 (2017).
- [23] V. Giovannetti, S. Lloyd, and L. Maccone, *Nature Photon* **5**, 222 (2011).
- [24] M. Beau and A. del Campo, *Physical Review Letters* **119**, 010403 (2017).
- [25] J. Maldacena, S. H. Shenker, and D. Stanford, *J. High Energy Phys.* **2016**, 106 (2016).
- [26] A. I. Larkin and Y. N. Ovchinnikov, *Soviet Journal of Experimental and Theoretical Physics* **28**, 1200 (1969).
- [27] K. Hashimoto, K. Murata, and R. Yoshii, *J. High Energy Phys.* **2017**, 138 (2017).
- [28] M. Hanada, H. Shimada, and M. Tezuka, *Phys. Rev. E* **97**, 022224 (2018).
- [29] H. Gharibyan, M. Hanada, B. Swingle, and M. Tezuka, *J. High Energy Phys.* **2019**, 82 (2019).
- [30] T. Akutagawa, K. Hashimoto, T. Sasaki, and R. Watanabe, *J. High Energy Phys.* **2020**, 13 (2020).
- [31] B. Kobrin, Z. Yang, G. D. Kahanamoku-Meyer, C. T. Olund, J. E. Moore, D. Stanford, and N. Y. Yao, *Phys. Rev. Lett.* **126**, 030602 (2021).
- [32] E. B. Rozenbaum, S. Ganeshan, and V. Galitski, *Phys. Rev. Lett.* **118**, 086801 (2017).
- [33] H. Shen, P. Zhang, R. Fan, and H. Zhai, *Phys. Rev. B* **96**, 054503 (2017).
- [34] N. Tsuji, T. Shitara, and M. Ueda, *Phys. Rev. E* **97**, 012101 (2018).
- [35] L. M. Sieberer, T. Olsacher, A. Elben, M. Heyl, P. Hauke, F. Haake, and P. Zoller, *npj Quantum Inf* **5**, 1 (2019).
- [36] E. M. Fortes, I. García-Mata, R. A. Jalabert, and D. A. Wisniacki, *Phys Rev E* **100**, 042201 (2019).
- [37] J. Chávez-Carlos, B. López-del Carpio, M. A. Bastarrachea-Magnani, P. Stránský, S. Lerma-Hernández, L. F. Santos, and J. G. Hirsch, *Phys. Rev. Lett.* **122**, 024101 (2019).
- [38] A. Keles, E. Zhao, and W. V. Liu, *Phys. Rev. A* **99**, 053620 (2019).
- [39] R. J. Lewis-Swan, A. Safavi-Naini, J. J. Bollinger, and A. M. Rey, *Nat. Commun.* **10**, 1581 (2019).
- [40] S. PG, V. Madhok, and A. Lakshminarayan, *J. Phys. D: Appl. Phys.* **54**, 274004 (2021).
- [41] S. Pilatowsky-Cameo, J. Chávez-Carlos, M. A. Bastarrachea-Magnani, P. Stránský,

- S. Lerma-Hernández, L. F. Santos, and J. G. Hirsch, *Phys. Rev. E* **101**, 010202 (2020).
- [42] Z. Wang, J. Feng, and B. Wu, *Phys. Rev. Research* **3**, 033239 (2021).
- [43] C. Yin and A. Lucas, *Phys. Rev. A* **103**, 042414 (2021).
- [44] A. Kitaev, “Hidden Correlations in the Hawking Radiation and Thermal Noise,” (2014), talk given at Fundamental Physics Prize Symposium.
- [45] J. Kurchan, *J. Stat. Phys.* **171**, 965 (2018).
- [46] N. Tsuji, T. Shitara, and M. Ueda, *Phys. Rev. E* **98**, 012216 (2018).
- [47] G. J. Turiaci, *J. High Energy Phys.* **2019**, 99 (2019).
- [48] C. Murthy and M. Srednicki, *Phys. Rev. Lett.* **123**, 230606 (2019).
- [49] S. Kundu, *J. High Energ. Phys.* **2022**, 10 (2022).
- [50] S. Pappalardi and J. Kurchan, *SciPost Physics* **13**, 006 (2022).
- [51] S. Pappalardi, L. Foini, and J. Kurchan, *SciPost Physics* **12**, 130 (2022).
- [52] S. Grozdanov, *Phys. Rev. Lett.* **126**, 051601 (2021), publisher: American Physical Society.
- [53] M. Heyl, A. Polkovnikov, and S. Kehrein, *Phys. Rev. Lett.* **110**, 135704 (2013), publisher: American Physical Society.
- [54] J. L. F. Barbón and E. Rabinovici, *J. High Energy Phys.* **2003**, 047 (2003).
- [55] J. Barbón and E. Rabinovici, *Fortschritte der Physik* **52**, 642 (2004).
- [56] K. Papadodimas and S. Raju, *Phys. Rev. Lett.* **115**, 211601 (2015).
- [57] J. S. Cotler, G. Gur-Ari, M. Hanada, J. Polchinski, P. Saad, S. H. Shenker, D. Stanford, A. Streicher, and M. Tezuka, *J. High Energ. Phys.* **2017**, 118 (2017).
- [58] J. Cotler, N. Hunter-Jones, J. Liu, and B. Yoshida, *J. High Energy Phys.* **2017**, 48 (2017).
- [59] M. L. Mehta, *Random Matrices* (Elsevier/Academic Press, 2004).
- [60] F. Haake, M. Kuś, and R. Scharf, *Z. Physik B - Condensed Matter* **65**, 381 (1987).
- [61] B. Bertini, P. Kos, and T. Prosen, *Physical Review Letters* **121**, 264101 (2018).
- [62] Z. Xu, L. P. García-Pintos, A. Chenu, and A. del Campo, *Phys. Rev. Lett.* **122**, 014103 (2019).
- [63] A. del Campo and T. Takayanagi, *J. High Energy Phys.* **2020**, 170 (2020).
- [64] Z. Xu, A. Chenu, T. Prosen, and A. del Campo, *Phys. Rev. B* **103**, 064309 (2021).
- [65] J. Cornelius, Z. Xu, A. Saxena, A. Chenu, and A. del Campo, *Phys. Rev. Lett.* **128**, 190402 (2022).
- [66] R. E. Prange, *Phys. Rev. Lett.* **78**, 2280 (1997).
- [67] F. Calogero, *Journal of Mathematical Physics* **12**, 419 (2003), publisher: American Institute of PhysicsAIP.
- [68] B. Sutherland, *J. Math. Phys.* **12**, 246 (1971), publisher: American Institute of Physics.
- [69] P. Claus, M. Derix, R. Kallosh, J. Kumar, P. K. Townsend, and A. Van Proeyen, *Phys. Rev. Lett.* **81**, 4553 (1998), publisher: American Physical Society.
- [70] G. W. Gibbons and P. K. Townsend, *Physics Letters B* **454**, 187 (1999).
- [71] O. Lechtenfeld and S. Nampuri, *Physics Letters B* **753**, 263 (2016).
- [72] F. D. M. Haldane, *Phys. Rev. Lett.* **67**, 937 (1991), publisher: American Physical Society.
- [73] Y.-S. Wu, *Phys. Rev. Lett.* **73**, 922 (1994), publisher: American Physical Society.
- [74] M. V. N. Murthy and R. Shankar, *Phys. Rev. Lett.* **73**, 3331 (1994), publisher: American Physical Society.
- [75] J. Jaramillo, M. Beau, and A. d. Campo, *New J. Phys.* **18**, 075019 (2016), publisher: IOP Publishing.
- [76] A. d. Campo, *New J. Phys.* **18**, 015014 (2016), publisher: IOP Publishing.
- [77] E. P. Wigner, *Mathematical Proceedings of the Cambridge Philosophical Society* **47**, 790 (1951).
- [78] E. P. Wigner, in *Conference on neutron physics by time-of-flight* (1956) pp. 1–2.
- [79] A. Chenu, I. L. Egusquiza, J. Molina-Vilaplana, and A. del Campo, *Sci. Rep.* **8**, 12634 (2018).
- [80] A. Chenu, J. Molina-Vilaplana, and A. del Campo, *Quantum* **3**, 127 (2019).
- [81] O. Bohigas, M. J. Giannoni, and C. Schmit, *Phys. Rev. Lett.* **52**, 1 (1984).
- [82] O. Bohigas, M. J. Giannoni, and C. Schmit, *J. Physique Lett.* **45**, 1015 (1984).

- [83] M. Kuś, R. Scharf, and F. Haake, *Z. Physik B - Condensed Matter* **66**, 129 (1987).
- [84] R. Scharf, B. Dietz, M. Kuś, F. Haake, and M. V. Berry, *EPL* **5**, 383 (1988).
- [85] F. Haake and D. L. Shepelyansky, *EPL* **5**, 671 (1988).
- [86] R. F. Fox and T. C. Elston, *Phys. Rev. E* **50**, 2553 (1994).
- [87] S. Chaudhury, A. Smith, B. E. Anderson, S. Ghose, and P. S. Jessen, *Nature* **461**, 768 (2009).
- [88] F. Haake, *Quantum Signatures of Chaos* (Springer Berlin Heidelberg, 2010).
- [89] J. Wang and J. Gong, *Phys. Rev. Lett.* **102**, 244102 (2009).
- [90] J. Wang and J. Gong, *Phys. Rev. E* **81**, 026204 (2010).
- [91] K. Bhattacharyya, *J. Phys. A: Math. Gen.* **16**, 2993 (1983).
- [92] S. A. Hartnoll and A. P. Mackenzie, “Planckian Dissipation in Metals,” (2022), arXiv:2107.07802 [cond-mat, physics:hep-th].
- [93] S. Grozdanov, *Physical Review Letters* **126**, 051601 (2021).